A Microwave OTA Using a Feedforward-Regulated Cascode Topology

You Zheng and Carlos E. Saavedra
Department of Electrical and Computer Engineering
Queen's University
Kingston, ON, Canada
Email: Carlos.Saavedra@queensu.ca

***Abstract*—A CMOS operational transconductance amplifier (OTA) with a novel feedforward-regulated cascode topology is proposed and experimentally demonstrated in this paper. It enables high-speed operation of the proposed OTA up to 8 GHz. For demonstration purposes, a microwave variable resistor and a variable active inductor using this OTA were fabricated using 0.18 μm CMOS process. Experimental results show that this OTA has a relatively high transconductance of about 10.5 mA/V at frequencies up to 8 GHz, with a tuning ratio of 1:5.3. The fabricated active inductor can achieve over 4.7 nH inductance at GHz frequencies and an inductance tuning ratio of 1:3.6 for microwave applications. The OTA basic cell integrated circuit measures 145 x 67 μm², excluding bonding pads.**

I. INTRODUCTION

Operational transconductance amplifiers (OTA) have been deemed as good candidates to replace the operational amplifier in high-frequency analog applications [1][2]. It has been demonstrated that OTAs are capable of implementing not only all of the functions of the operational amplifier from summation and integration to high-order filtering functions, but also other functions with great simplicity, such as variable resistors and variable active inductors [2]. In cases where power consumption considerations are not very stringent, active inductors have received significant attention in RF and microwave integrated circuit (RFIC/MIC) applications, due to their potential to significantly increase the circuits' Q factor and reduce the space used by passive inductors [3].

To realize high-frequency active inductors, a high-speed OTA is the key element. Some previously-developed CMOS OTA topologies [4] used current mirrors to combine their output currents in order to achieve high transconductance, but they could only work at low RF frequencies because of the time delay introduced by the current mirrors and the large parasitics associated to the complicated topologies. A single NMOS common-source amplifier in contrast is the simplest transconductor with the least parasitics. However, multiple drawbacks come with this single-transistor transconductor and deviate it from a very useful OTA, such as its relatively low output impedance, its Miller effect due to its input-output coupling [5] and its nonlinearity. The nonlinearity mainly degrades the OTA's large-signal performance.

To alleviate these problems, some cascode topologies have been suggested for the OTAs [4]. A basic cascode topology introduces an additional common-gate transistor at the top of the original common-source transistor to create isolation between its input and output, and therefore increases its output impedance and reduces the Miller effect [5]. The additional transistor also helps to stabilize the drain voltage of the original transistor, which increases the linearity of the transconductance [6][7]. The basic cascode topology improves the OTA performance approximately by a factor of $g_{m2}r_2$ compared to the single common-source transconductor, where g_{m2} and r_2 are the additional transistor's transconductance and drain-source resistance in its saturation region [9]. A regulated cascode topology is an enhanced cascode topology [4][9]. It applies a local negative feedback $(-A)$ to the additional transistor to further regulate and stabilize the drain voltage of the original transistor, which improves the OTA performance approximately by a factor of $Ag_{m2}r_2$, i.e. A times that of the basic cascode topology [7]. The local feedback network can be implemented using a common-source amplifier [9] or an additional differential OTA [7]. The later configuration can provide higher feedback gain for the regulation, but at the expense of more complicated circuitry and slower regulation. At high frequencies, the slow regulation could cancel the performance improvement from the regulated cascode, and in the worst case, deteriorate the cascoding performance.

A very high-speed OTA using a feedforward-regulated cascode topology is presented and experimentally demonstrated in this work. The feedforward configuration instead of the local feedback configuration enables fast regulation with the cascode topology, and thus can achieve high speed for the proposed OTA. As its applications, a variable resistor and a variable active inductor were then implemented to demonstrate this OTA's performance. Their simulation and measurement results are both presented in this work. The rest of this paper is organized as follows. The proposed feedforward-regulated cascode OTA topology is described in Section II and the applications of the proposed OTA are presented in Section III. Experimental results from the fabricated integrated circuits together with the simulation results are presented and discussed in Section IV. Section V concludes this paper.

1-4244-0921-7/07 $25.00 © 2007 IEEE.

II. FEEDFORWARD-REGULATED CASCODE OTA

The proposed CMOS OTA with a feedforward-regulated cascode topology is presented in Fig. 1(a). It is a CMOS differential configuration, which is favourable for most OTA circuits, because the differential inputs can facilitate both positive feedback and negative feedback that are often required in these circuits [2]. The OTA in Fig. 1(a) contains two PMOS regulated cascodes (T_1/T_2 and T_5/T_6) and two NMOS regulated cascodes (T_3/T_4 and T_7/T_8), where the PMOS cascodes have the same configuration as the NMOS cascodes and their DC currents are controlled by the two current sources at the bottom. The current sources are implemented simply using two NMOS transistors with a control voltage V_c. Instead of the local negative feedback, the OTA in Fig. 1(a) uses negative feedforwards for its four cascodes to speed up the regulating process. They are realized by two pairs of cross connections between the two PMOS cascodes and the two NMOS cascodes, which also work as the coupling between the two differential paths, as illustrated in Fig. 1(a). To simplify the explanation of the feedforward configuration, Fig. 1(b) shows only one pair of the connections between the right PMOS cascode and the left NMOS cascode. Here we assume that a large differential signal (V_{in}+ and V_{in}-) is fed to the OTA, e.g. V_{in}+ is at its high voltage with its signal polarity of (+) and V_{in}- is at its low voltage with its signal polarity of (-) in Fig. 1(b). If the cross connections did not exist this large differential signal would cause a decrease of the drain voltage V_{d4} of the transistor T_4 and an increase of the drain voltage V_{d5} of the transistor T_5 (marked with their signal polarities in Fig. 1(b)). The changes of the two drain voltages would decrease the linearity of the transistors T_4 and T_5 [6][7]. With the cross connections, however, these drain-voltage changes also cause an increase of the gate-source voltages of the transistors T_3 and T_6. It increases their drain-source currents to reduce the changes of the drain voltages V_{d4} and V_{d5}. Therefore, the drain voltages V_{d4} and V_{d5} are kept stable through this process even if there is a large input signal. The other two cascode PMOS and NMOS transconductors not presented in Fig. 1(b) perform the same way as described here. Because the regulating voltage of each cascode transconductor comes from the other differential input, these regulating voltages are called negative feedforward rather than negative feedback here.

The previous local negative feedback [4][9] senses the drain voltage that is going to be regulated by the feedback, so it always introduces delay in its voltage regulation from the negative feedback network. However, in the OTA proposed here, the feedforward can completely remove the regulating delay if V_{d4} and V_{d5} in Fig. 1(b) change at the same time, which can be attained by properly selecting the width ratio between the PMOSFETs and the NMOSFETs. As discussed in Section I, fast regulation helps to speed up the operation of the proposed OTA, which will be demonstrated in Section IV. The use of CMOS configuration here has some benefits such as symmetric output-signal swing and high transcondutance. Moreover, when it is applied in OTA circuits, it saves space because the CMOS OTA output can be directly applied to other OTA's inputs or its own inputs without any DC blocks or bias circuits. Therefore, the circuits' complexity can be significantly reduced.

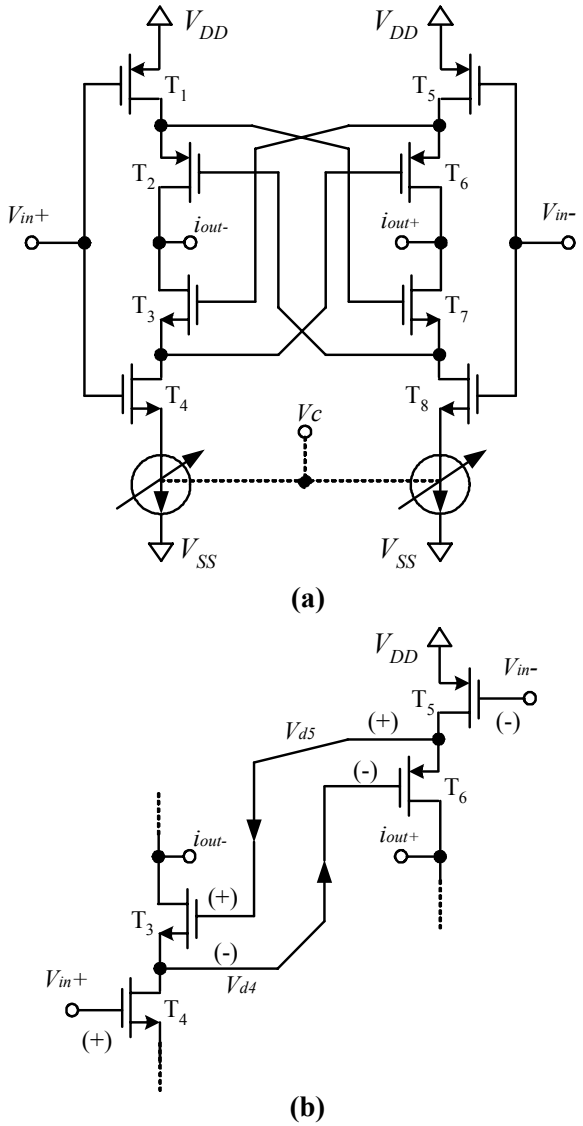

Figure 1. (a) The propose CMOS differential OTA using negative feedforward-regulated cascodes, (b) and its one pair of cross connections.

III. FEEDFORWARD-REGULATED CASCODE OTA CIRCUIT APPLICATIONS

A variable resistor and a single-ended active inductor were implemented using the proposed high-speed OTA, in order to test its performance. It is known that an OTA's transcondutance can be easily characterized at low frequencies by dividing the measured output current by the measured input voltage, while at microwave frequencies, direct measurement of either voltage or current is difficult. Indirect methods have to be used to perform this characterization. The implemented variable resistor shown in Fig. 2(a) is one of these methods and it is adopted in this

work to help to characterize the OTA's transconductance. According to [2], a direct connection of the non-inverting output of a differential variable OTA (g_m) to its inverting input can compose a variable resistor, with its input resistance equaling to

$$R_{in} = 1/g_m \tag{1}$$

This resistance can be calculated from the input admittance (Y_{in}) derived from the measured input reflection coefficient (S_{11}) of the variable resistor

$$R_{in} = 1/\mathrm{Re}(Y_{in}) \tag{2}$$

Therefore the OTA's transconductance g_m can be attained from the S-parameter measurement of the variable resistor according to (1) and (2). Moreover, the input/output parasitic capacitances of the OTA can be predicted from the imaginary part of Y_{in}.

The single-ended variable active inductor was implemented using the common topology [2] shown in Fig. 2(b), without any DC block or bias circuit for its feedback networks because of the aforementioned CMOS configuration of the proposed OTA. Two identical OTAs are adopted in implementing this active inductor. The capacitor C shown in Fig. 2(b) is formed by the OTAs' input/output parasitic capacitance. The active inductance is given by [2]

$$L = C/g_m^2 \tag{3}$$

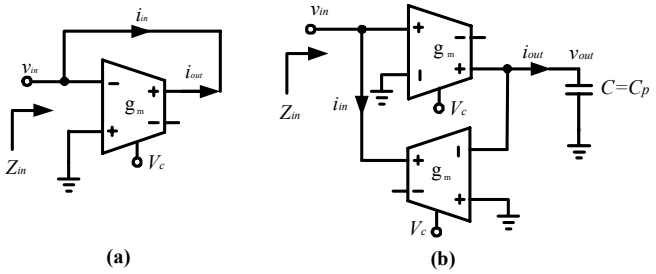

Figure 2. The block diagrams of the implemented (a) variable resistor and (b) active inductor.

IV. Simulation and Measurement Results

The implemented variable resistor and variable active inductor were fabricated using 0.18 μm CMOS technology. The used OTA basic cell measures 145x67 μm^2. Fig. 3 shows a microphotograph of the fabricated circuits under test. The variable resistor and the active inductor were measured through the coplanar-waveguide (CPW) pads on the left side and on the right side respectively. The DC supplies used in the measurement were V_{DD}=1.4V and V_{SS}=-1.4V.

Using the method described in Section III, the OTA's transconductance and its input/output capacitance were

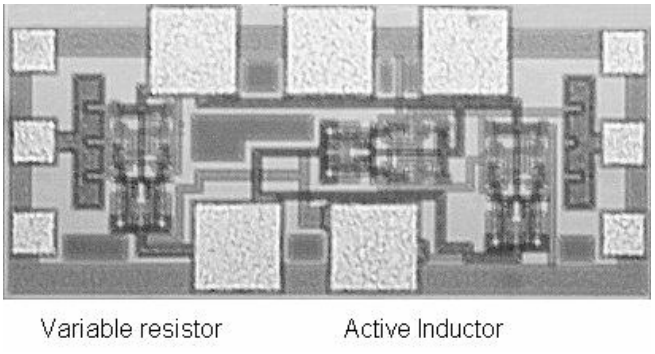

Figure 3. A microphotograph of the fabricated variable resistor and active inductor.

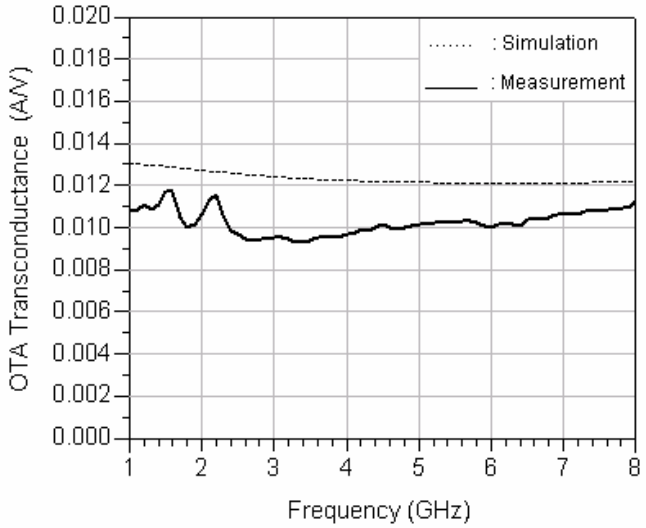

Figure 4. The proposed OTA's transconductance (V_c=-0.55V).

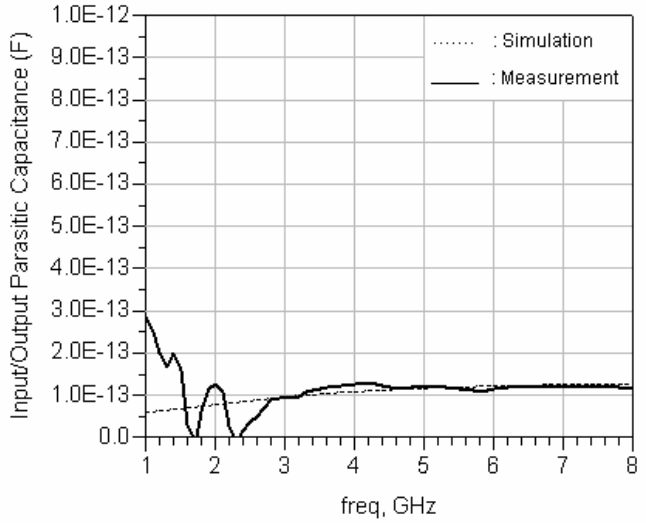

Figure 5. The input/output parasitic capacitance of the proposed OTA (V_c=-0.55V).

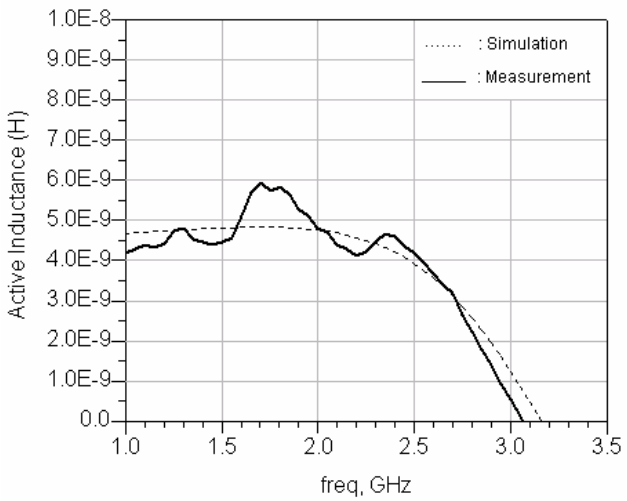

Figure 6. The indutance of the active inductor (V_c=-0.55V).

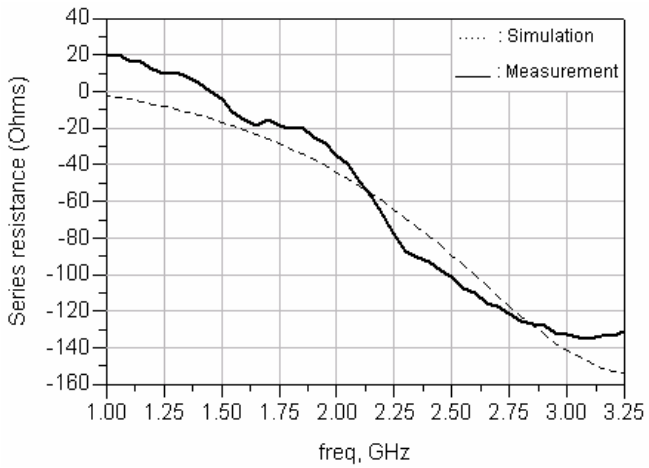

Figure 7. The series resistance of the active inductor (V_c=-0.55V).

calculated from the measurement, as shown in Fig. 4 and Fig. 5. The simulation results are also included in these two figures for comparison and the agreement is excellent. As shown in Fig. 4, the fabricated OTA can achieve a relatively large transconductance of about 10.5 mA/V with a small variation of ±1mA/V throughout an ultra-wide band from 1 GHz up to 8 GHz, at a control voltage of V_c=-0.55V. The simulation also gives a wideband transconductance of about 12.5mA/V, which is close to the measured transconductance. The transconductance can be tuned from 2 mA/V to 10.5mA/V, a tuning ratio of about 1:5.3, through the control voltage V_c. The DC power consumption of this OTA varies from 2.5 mW to 35.6 mW in this tuning. The input/output parasitic capacitance of the fabricated OTA is about 0.1pF from Fig. 5, which is well predicted by the simulation. Moreover, the common-mode-rejection-ratio (CMRR), the power-supply-rejection-ratio (PSRR+ and PSRR-), and the third-order-inter-modulation (IM3) suppression of the OTA are also simulated. The CMRR is 85.5 dB at 10 MHz and 36.7 dB at 4 GHz. The PSRR+ (PSRR-) is 90.4 dB (86.2 dB) at 10 MHz and 41.5 dB (36.9 dB) at 4 GHz. The IM3 suppressions (1.0 V_{pp} input) at these two frequencies are 42.8 dBc and 46.0 dBc respectively.

Fig. 6 and Fig. 7 show the inductance and the series resistance of the fabricated active inductor both from the simulation and measurement, where the simulation also well predicts the measurement results. The active inductor can achieve an inductance of about 4.7nH at the control voltage of V_c=-0.55V. The active inductance varies with the control voltage V_c. A maximum inductance of 17nH was measured at a control voltage of V_c=-0.66V, resulting in an inductance tuning ratio of 1:3.6. The self-resonant frequency of the active inductor is about 3.1 GHz as seen in Fig. 6. Because of the relatively large transconductance and the existing phase lag of the OTA [10], this active inductor can achieve zero series resistance or even negative series resistance (shown in Fig. 7) by tuning the control voltage V_c. Therefore, high-Q circuits can be realized using this active inductor, without any extra negative-impedance-circuit (NIC). The NIC is usually used to compensate for losses in circuits such as a voltage-controlled oscillator or an active filter, which however could reduce their operational frequencies [3].

V. CONCLUSION

The proposed feedforward-regulated cascode OTA can work in an ultra-wide band with a large transconductance tuning range, which makes it very suitable for implementing high-Q RF/microwave integrated circuits using CMOS technology.

REFERENCES

[1] T. Deliyannis, Yichuang Sun and J.K. Fidler, *Continuous-Time Active Filter Design*, CRC Press, 1999.

[2] Randall L. Geiger and Edgar Sanchez-Sinencio, "Active filter design using operational transconductance amplifiers: A tutorial," *IEEE Circuit and Device Magazine*, 1985.

[3] Yue Wu, Xiaohui Ding, Mohammed Ismail and Hakan Olsson, "RF bandpass filter design based on CMOS active inductors," *IEEE Transactions on Circuit and Systems – II: Analog and Digital Signal Processing*, vol.50, pp.942-949, Dec. 2003.

[4] E. Sanchez-Sinencio and J. Silva-Martinez, "CMOS transconductance amplifiers, architectures and active filters: a tutorial," *IEEE Trans. on Circuits and Systems I: Fundamental Theory and Applications*, vol. 48, pp.1138-1141, Sept. 2001.

[5] Thomas H. Lee, *The Design of CMOS Radio-Frequency Integrated Circuit*s, Cambridege University Press, 1998, pp.203-206.

[6] J. L. PENNOCK, "CMOS triode transconductor for continuous-time active integrated filters," *Electronics Letters*, vol.21, pp.817-818, 1985.

[7] A. Wysynski, "Low-voltage CMOS and BiCMOS triode transconductors and integrators with gain enhanced linearity and output impedance," *Electronics Letters*, vol.30, pp.211-212, 1994.

[8] A. S. Sedra and K. C. Smith, *Microelectronic Circuits*, Oxford University Press, 1998, pp.533-535.

[9] E. Sackinger and W. Guggenbuhl,"A high-swing, high impendance MOS cascode circuit," *IEEE Journal of Solid-State Circuits*, pp.289-298, 1990.

[10] Haiqiao Xiao, Rolf Schaumann, etal., "A radio-frequency CMOS active inductor and its application in designing high-Q filters," *Proceedings of the 2004 International Symposium on Circuits and Systems*, vol. 4, pp. 197-200, 2004.